Molecular modelling of entanglement

BY MASAO DOI AND JUN-ICHI TAKIMOTO

*Department of Computational Science and Engineering,
Nagoya University, Nagoya, Japan*

The modelling of molecular entanglement in polymeric materials is an old problem, and has evolved gradually over the last 60 years, with two key approaches: the network model of Green & Tobolsky, and the tube model of Edwards and de Gennes. We will show that these models can be merged together in a straightforward manner. The resulting model, called the dual slip-link model, can be handled by computer simulation, and it can predict the linear and nonlinear rheological behaviours of linear and star polymers with arbitrary molecular weight distribution.

**Keywords: viscoelasticity; entanglement junction; reptation; tube model;
temporary network model; dual slip-link model**

1. Introduction

Molecular modelling of entanglement in polymeric materials is an old problem: when Staudinger (1932) proposed that polymers are long chain-like molecules, he must have realized that such molecules entangle with each other. The molecular entanglement is an important problem, as it is closely related to the characteristic property of polymeric materials, namely, the viscoelasticity.

The unvulcanized rubber which is sold at stationery stores is a soft elastic rubbery material, but it is actually a liquid; it can flow under constant load and can be moulded into any shape. Polymeric liquids (the molten state of un-cross-linked polymers) generally have this property. They behave like an elastic rubber at short times, while they flow like a liquid if they are subjected to a stress for a long time.

Such behaviour can be understood at least qualitatively from the molecular viewpoint. A polymeric liquid is made of many chain-like molecules entangling with each other. When such a material is deformed quickly, each molecule is deformed and generates a restoring force. This corresponds to the rubbery response for fast deformation. On the other hand, the restoring force will decrease in time as the deformation of the molecule relaxes. Due to the molecular entanglement, the relaxation takes an extremely long time (from seconds to hours). An important objective in physics (and engineering) is to understand and to predict such behaviour from a knowledge of the fluid's molecular structure.

Though the effect of entanglement is easy to understand, theoretical modelling of entanglement is not so easy, and the modelling of entanglement has some history.

The first modelling of entanglement was made by Green & Tobolsky (1946), around 10 years after the molecular theory of rubber elasticity was proposed by Kuhn. Green

One contribution of 14 to a Discussion Meeting 'Slow dynamics in soft matter'.

& Tobolsky regarded the polymeric liquid as a network of polymers made of 'entanglement junctions'. Unlike the chemical junctions in rubbers, the entanglement junctions are dynamical, and they are constantly created and destroyed due to random molecular motion. Green & Tobolsky made assumptions for the creation and destruction rate for the entanglement junctions, and they derived a rheological constitutive equation for unvulcanized rubber. Their constitutive equation did not work very well, as the assumptions they made were too simple, but the theory became the basis of the subsequent development of the rheological properties of polymeric liquids.

Many modifications have been made to the theory of Green & Tobolsky to make the resulting constitutive equations agree with experiments (Lodge 1974; Bird *et al*. 1987). These modifications were useful but, as they were made from phenomenological view points, the theories did not have much predictive power; for example, the theories could not predict how the material properties depend on the molecular weight of polymers.

A new model of entanglement was marked by the celebrated papers of Edwards (1967) and de Gennes (1971). They proposed that each polymer in the entangled state can move in a tube-like region which surrounds the polymer. The tube is regarded as fixed in the material, but its shape changes in time as the two ends of the chain can evacuate the old tube and create a new segment of tube. This model was applied to the problem of rheology by Doi & Edwards (1978, 1986) and explained many characteristic features of the viscoelasticity of polymeric liquids with a small number of parameters. The theory, however, failed in many respects. For example, it failed to predict the behaviour of the polydisperse system properly, and it gave an incorrect prediction for the steady shear flow: according to the original model, the shear stress has a maximum as a function of the shear rate.

Various effects have been introduced to resolve these failures. The most important effect is 'constraint release', which arises from the motion of surrounding polymers (de Gennes 1976). Doi & Edwards considered that each tube represents the average constraint imposed by the surrounding polymers, and they assumed that it is fixed in the material. In fact, the tube is a mobile object, since the constraint imposed by the surrounding polymers will change due to their own motion: a constraint will disappear if a surrounding polymer goes away. This effect introduces various modifications in the original tube model, such as 'double reptation' (des Cloizeaux 1988), 'dynamical tube dilation' (especially in star polymers) (Ball & McLeish 1989), and convective constraint release (Marrucci 1996; Ianniruberto & Marrucci 1996; Milner *et al*. 2001). These modifications greatly improved the predictive power of the theory but, as they are introduced in different contexts, it gradually became increasingly difficult to take all effects into account in one framework.

Recently, we formulated the problem of constraint release in a simple model, called the dual slip-link model (Takimoto *et al*. 2000). The model takes into account all the effects discussed above and can handle their cumulative effect in a consistent way. Here we describe the model and discuss some of its results.

2. Dual slip-link model

Figure 1 shows the conceptual picture of the dual slip-link model. The entanglement junction is represented by a slip link through which chains can pass freely. This representation is very much like the classical picture of an 'entanglement junction'
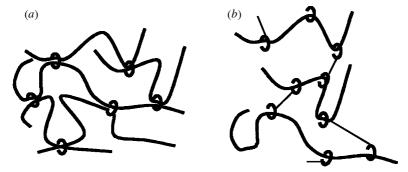
(*a*) (*b*)

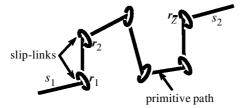Figure 1. (*a*) The dual slip-link model. (*b*) The dual slip-link model with virtual links.

Figure 2. Primitive path and slip links.

of Green & Tobolsky. However, the dual slip-link model is a development of the tube model and is more closely connected to it than the model of Green & Tobolsky.

As has been shown previously by Doi & Edwards (1978), the tube can equivalently be represented by slip links, by which each chain is confined, but through which it can slide freely. In their model, however, the slip link confines a single chain and is an alternative representation of the tube constraints. Therefore, the slip links are assumed to be created only at either end of the chain and destroyed only when the chain slides off it. In the dual slip-link model, on the other hand, the slip link confines a pair of chains. A slip link is destroyed if either of the chains slide off the slip link. The motivation for considering such a model is to take into account of the effect of constraint release for many-chain systems.

In the following we shall describe the simplest implementation of this idea. In this implementation, the slip link does not represents the entanglement junction in real space such as shown in figure 1*a*, but represents effective constraints whose statistical character is determined by the other polymers. A more straightforward implementation of the dual slip-link model is possible. Masubuchi *et al.* (2001) regarded the slip link as an actual link in real space, and they calculated the motion of the position of the slip-link points together with the reptation of the chains in the system. So far, however, results of this model have been similar to those described here.

3. Dual slip-link model with virtual links

The present model is based on the description of the tube model. The coformation of a polymer chain is represented by the primitive path: the set of the line segments starting from one end of the chain, connecting the neighbouring slip links and ending at the other end of the chain (see figure 2). The primitive path is represented by the position vectors of the slip links $(\boldsymbol{r}_1, \boldsymbol{r}_2, \ldots, \boldsymbol{r}_{\bar{Z}})$, and the lengths of the line segments

at both ends are s_1 and s_2, respectively. The number of slip links $\tilde{Z}$ in a chain is a statistical quantity, and its average in the equilibrium state $\langle \tilde{Z} \rangle$ is equal to the number of entanglement points $Z = M/M_e$, where M is the molecular weight of the chain and M_e is the entanglement molecular weight of this polymer. The equilibrium length of the primitive path is $L_{eq} = Za$, where a is the average distance between slip links.

In our simulation, many chains are generated in a computer. Each slip link is paired with its 'partner', which is randomly selected from slip links on other chains as is shown in figure 1b. These pairings represent binary entanglements among polymer chains. Each chain moves in its own three-dimensional space. In this model, the interaction among the chains is taken into account only through the pairing of the slip links.

At each time-step of the simulation, we carry out the following four operations.

(i) Affine deformation due to flow. Each position of the slip links $\boldsymbol{r}_i$ is displaced affinely according to the macroscopic flow applied to the sample.

(ii) Change of the contour length of the primitive path. The length L of each primitive path is updated to $L + \Delta L$ by changing the lengths of the tails s_1 and s_2 by the same amount, $\Delta L/2$. ΔL is determined from the following Langevin equation and the time-step Δt as

$$\frac{\mathrm{d}L}{\mathrm{d}t} = -\frac{1}{\tau_R}(L(t) - L_{eq}) + g(t) + \left(\frac{\mathrm{d}L}{\mathrm{d}t}\right)_{affine}. \tag{3.1}$$

Here, $(\mathrm{d}L/\mathrm{d}t)_{affine}$ is the change of the contour length due to the affine deformation, $g(t)$ is a random variable representing the contour length fluctuation, $\tau_R = \tau_e Z^2$ is the Rouse relaxation time, and τ_e is the unit of time (the Rouse relaxation time of a chain whose molecular weight is M_e).

(iii) Reptation. Each primitive path is randomly displaced along itself with the diffusion coefficient $D_c = a^2/(3\pi^2\tau_e Z)$. By this operation, either s_1 increases and s_2 decreases, or vice versa.

(iv) Constraint renewal. If s_1 (or s_2) becomes negative by operations (ii) and (iii), the last slip link on the chain and its partner are removed. If, on the other hand, s_1 (or s_2) becomes longer than a, a new slip link is created at the end, and its partner is created on a randomly selected chain.

For a given configuration of the chain, the stress is calculated by

$$\sigma_{\alpha\beta} = \frac{3k_B T}{a} \sum_i \left\langle \frac{r_{i\alpha} r_{i\beta}}{|\boldsymbol{r}_i|} \right\rangle, \tag{3.2}$$

where $\langle \cdots \rangle$ indicates the average for all chains.

A similar stochastic simulation method has been developed by Hua & Schieber (1998).

These operations are carried out for linear polymers. We have also conducted the simulation for star polymers. In the case of star polymers, the reptation process is absent. Hence we skipped operation (iii) and used only operations (i), (ii) and (iv). Within this model, the number of arms has no effect on the rheology of star polymers.
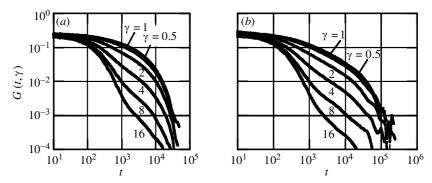
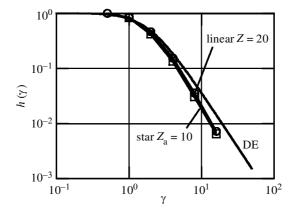Figure 3. Nonlinear relaxation moduli of (*a*) linear ($Z = 20$) and (*b*) star ($Z_a = 10$) polymers.

Figure 4. The damping function of linear and star polymers.

In the following, the stress, time and shear rate are measured in units of G_e, τ_e, and $1/\tau_e$, respectively. Here, the unit of stress is related to the plateau modulus G_N as $G_e = (15/4)G_N$.

4. Comparison between linear and star polymers

(*a*) *Stress relaxation*

Nonlinear stress relaxation moduli $G(t, \gamma)$ of linear ($Z = 20$) and star ($Z_a = 10$) polymers are shown in figure 3. The time-stress decoupling $G(t, \gamma) = h(\gamma)G(t)$ holds in the long-time region, and the resulting damping function $h(\gamma)$ is shown in figure 4. Although the linear relaxation modulus $G(t)$ is quite different for linear and star polymers, the damping function is almost identical for the two polymers. The value of $h(\gamma)$ obtained by our simulation is close to but slightly smaller than that predicted by the Doi–Edwards theory, because the present simulation takes account of the constraint release during the retraction of primitive paths to their equilibrium length.

(*b*) *Steady shear flow*

Figure 5 shows the shear stresses of linear polymers as a function of the shear rate. Note that the shear stress is a monotonously increasing function of the shear rate.
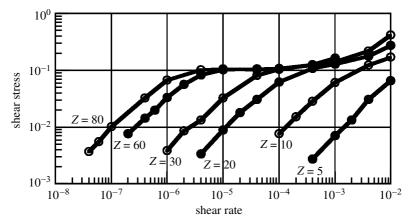
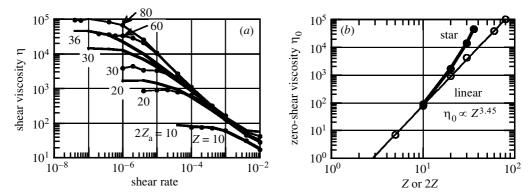Figure 5. Flow curves of linear polymers with various molecular weights.

Figure 6. Shear viscosities of linear and star polymers. (*a*) Non-newtonian viscosities: thin lines with symbols, linear polymers; thick lines, star polymers; (*b*) zero-shear viscosities.

This indicates that our method correctly takes account of the convective constraint release process (Marrucci 1996; Ianniruberto & Marrucci 1996). In the shear-rate range $1/\tau_{\rm d} < \dot\gamma < 1/\tau_{\rm R}$ ($\tau_{\rm d}$ is the longest relaxation time), the shear stress takes a constant value independent of the molecular weight. The constant value is *ca.* $0.10G_{\rm e}$, which is close to the theoretical value (0.123) of Mead *et al.* (1978).

Figure 6*a* shows the steady shear viscosity of linear and star polymers with various molecular weights. It is seen that, at high shear rate, linear and star polymers have the same viscosity, which is independent of the molecular weight in this shear-rate range. This is because, in the shear-rate range $1/\tau_{\rm d} < \dot\gamma < 1/\tau_{\rm R}$, the dominant relaxation mechanism is the convective constraint release, which is a local process equally effective for linear and star polymers.

Figure 6*b* shows the zero-shear viscosity η_0 of linear and star polymers. In the case of linear polymers, η_0 is proportional to $Z^{3.5}$, in good agreement with experiments. In the case of star polymers, the simulation results for $Z_{\rm a} \geqslant 10$ can be fitted by $\eta_0 \propto \exp(\alpha Z_{\rm a})$ with $\alpha \sim 0.4$. This is close to, but still differs significantly from, the value of 0.5 predicted by the dynamic-tube-dilation theory of Ball & McLeish (1989).
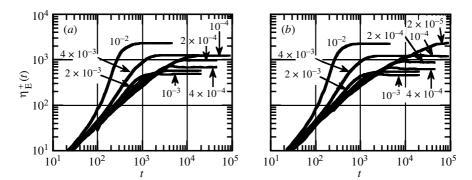
Figure 7. Elongational viscosities of monodisperse (*a*) linear ($Z = 20$)
and (*b*) star ($Z_a = 10$) polymers.

(*c*) *Elongational viscosity*

Figure 7 shows the time development of the elongational viscosity $\eta_E^+(t)$ when a uniaxial elongational flow is started. Figure 7*a* shows the result of a monodisperse linear polymer with $Z = 20$ entanglement points and figure 7*b* shows that of a star polymer with $Z_a = 10$ entanglement points per arm. The numbers in the figures are the dimensionless strain rate $\dot{\epsilon}\tau_e$. Except for the linear viscosity (the viscosity at the lowest strain rate), the elongational viscosity for linear and star polymers is quite similar. Especially, the strain hardening of $\eta_E^+(t)$ takes place in both polymers only when the strain rate $\dot{\epsilon}$ is larger than $1/\tau_R$, where the Rouse relaxation time of these polymers is $\tau_R = Z^2\tau_e = 4Z_a^2\tau_e = 400\tau_e$.

As it has been seen in this section, the linear viscoelasticity, such as the linear relaxation modulus $G(t)$, and the zero-shear viscosity η_0, for linear and star polymers, are quite different, because of the absence of reptation in star polymer. On the other hand, their nonlinear rheological properties, such as the damping function $h(\gamma)$, non-Newtonian viscosity $\eta(\dot{\gamma})$ or nonlinear elongational viscosity $\eta_E^+(t)$, are very similar to each other. This is because they are dominated by the Rouse relaxation and/or convective constraint release.

5. Dielectric relaxation

The molecular motion of polymers can be studied by dielectric relaxation. In the case of the type-A linear chain, which has dipole moments along its backbone, the dielectric relaxation function $\Phi(t)$ can be calculated from the auto-correlation function $\langle \boldsymbol{R}(t) \cdot \boldsymbol{R}(0) \rangle$ of the end-to-end vector $\boldsymbol{R}$. Matsumiya *et al.* (2000) have theoretically shown that, if dynamical tube dilation (Ball & McLeish 1989) is fully taking place during the relaxation, then the normalized stress relaxation function $g(t) \equiv G(t)/G(0)$ and dielectric relaxation function $\phi(t) \equiv \Phi(t)/\Phi(0)$ satisfy the relation $g(t) = [\phi(t)]^2$. They have also tested this relation experimentally and found that the relation actually holds for linear polymers.

To see whether such a relation is satisfied in our simulation, we have calculated $g(t)$ and $\phi(t)$ for linear polymer ($Z = 20$). The results are shown in figure 8*a*. It can be clearly seen that the calculated $g(t)$ and $\phi(t)$ satisfy the relation $g(t) = [\phi(t)]^2$.

The (normalized) storage and loss moduli $G'(\omega)$ and $G''(\omega)$, and the imaginary part of the dielectric function $\epsilon''(\omega)$ are calculated from $g(t)$ and $\phi(t)$ by Fourier
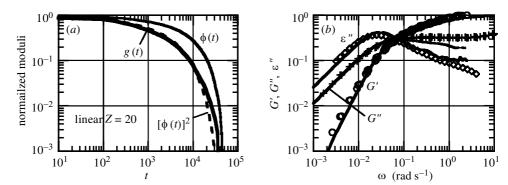
Figure 8. (*a*) Stress and dielectric relaxation moduli of linear polymer; (*b*) dynamic moduli and dielectric function. Symbols denote experiments and lines denote simulation.
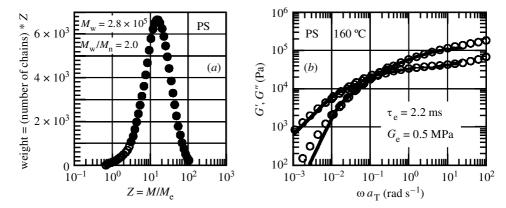

Figure 9. Polydisperse polystyrene sample. (*a*) Molecular weight distribution; (*b*) dynamic moduli: symbols, experiment; lines, simulation.

transform. The results are compared with experiments of Matsumiya *et al.* (2000) in figure 8*b*. The agreement with the experiments is very good, showing that the effect of dynamic tube dilation is correctly accounted for in our simulation.

6. Elongational viscosity of polydisperse system

Controlling the elongational viscosity of polymer melts is of great practical importance in polymer engineering, because it governs the processability of the polymer in blow and film moulding. In this section, we apply our model to predict the elongational viscosity of polydisperse samples. The sample we studied is a commercial polystyrene whose molecular weight distribution is shown in figure 9*a*. The data are plotted against $Z = M/M_e$, where the entanglement molecular weight M_e of polystyrene is taken to be $14\,500$ g mol^{-1}. About $10\,000$ chains obeying this molecular weight distribution are used in the simulation. The components of very short chains (chains shorter than $Z = 3$) are ignored in the simulation.

Before studying the elongational viscosity, we should determine the two model parameters τ_e and G_e corresponding to this sample and the measurement temperature of 160 °C. (Strictly speaking, G_e should be related to M_e as $G_e = (15/4)G_N =$
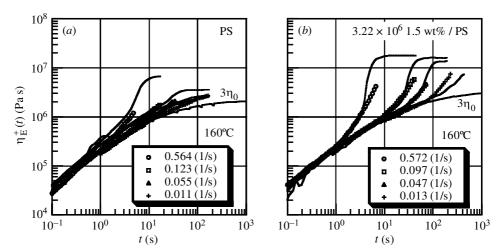
Figure 10. Elongational viscosities of polydisperse polystyrene samples: (*a*) base sample; (*b*) with 1.5 wt % of very high molecular weight component.

$3\rho RT/M_e \sim 0.6$ MPa, but we take G_e as an independent parameter from M_e.) To determine G_e and τ_e, stress relaxation modulus $G(t)$ after small step strain ($\gamma = 0.5$) is calculated by simulation, and is converted to the dynamic moduli $G'(\omega)$ and $G''(\omega)$ by Fourier transform. By fitting $G'(\omega)$ and $G''(\omega)$ to the experimental data of Minegishi *et al.* (2001), the parameters are determined to be $\tau_e = 2.2$ ms and $G_e = 0.5$ MPa. The agreement with the experiments is fairly good, as can be seen in figure 9*b*.

Uniaxial elongational viscosity of this sample at various strain rates is then calculated using our simulation and compared with experiments in figure 10*a*. Although there are no adjustable parameters, the agreement is very good.

To study the effect of a small amount of very high molecular weight component on the strain hardening of elongational viscosity, Minegishi *et al.* (2001) have blended 5 wt % of very long chains (molecular weight of 3220 kg mol^{-1}, or $Z = 222$) with the polystyrene sample. Figure 10*b* shows the elongational viscosity of the blend, compared with the prediction of our simulation. The strain hardening is strongly enhanced by 5 wt % of very long chains, and the enhancement is correctly predicted by our simulation.

7. Conclusion

The dual slip-link model is a straightforward generalization of the slip-link representation of the tube model, but it can also take into account the various effects discussed previously (double reptation, dynamic tube dilation and convective constraint release) in a simple and consistent way. The model can handle polydisperse systems and can reproduce the linear and nonlinear rheological properties of linear and star polymers accurately. The simulation program shown here is called PASTA, and can be downloaded at http://www.octa.jp.

References

Ball, R. C. & McLeish, T. C. B. 1989 Dynamic dilution and the viscosity of star-polymer melts. *Macromolecules* **22**, 1911–1913.

Bird, R. B., Curtiss, C. F., Armstrong, R. C. & Hassager, O. 1987 *Dynamics of polymeric liquids*, vol. 2. Wiley.

de Gennes, P.-G. 1971 Reptation of a polymer chian in the presence of fixed obstacles. *J. Chem. Phys.* **55**, 572–579.

de Gennes, P.-G. 1976 Dynamics of entangled polymer solutions. I. The Rouse model. *Macromolecules* **9**, 587–593.

des Cloizeaux, J. 1988 Double reptation vs simple reptation in polymer melts. *Europhys. Lett.* **5**, 437–442.

Doi, M. & Edwards, S. F. 1978 Dynamics of concentrated polymer systems. *J. Chem. Soc. Faraday Trans. 2* **74**, 1802–1817.

Doi, M. & Edwards, S. F. 1986 *The theory of polymer dynamics*. Oxford University Press.

Edwards, S. F. 1967 The statistical mechanics of polymerized material. *Proc. Phys. Soc.* **92**, 9–16.

Green, M. S. & Tobolsky, A. V. 1946 A new approach to the theory of relaxing polymer media. *J. Chem. Phys.* **14**, 80–92.

Hua, C. C. & Schieber, J. D. 1998 Segment connectivity, chain-length breathing, segmental stretch, and constraint release in reptation models. I. Theory and single-step strain predictions. *J. Chem. Phys.* **109**, 10 018–10 027.

Ianniruberto, G. & Marrucci, G. 1996 On compatibility of the Cox–Merz rule with the model of Doi and Edwards. *J. Non-Newton. Fluid Mech.* **65**, 241–246.

Lodge, A. S. 1974 *Elastic liquids*. Academic.

Marrucci, G. 1996 Dynamics of entanglements: a nonlinear model consistent with the Cox–Merz rule. *J. Non-Newton. Fluid Mech.* **62**, 279–289.

Masubuchi, Y., Takimoto, J., Koyama, K., Ianniruberto, G., Greco, F. & Marrucci, G. 2001 Brownian simulations of a network of reptating primitive chains. *J. Chem. Phys.* **115**, 4387–4394.

Matsumiya, Y., Watanabe, H. & Osaki, K. 2000 Comparison of dielectric and viscoelastic relaxation functions of cis-polyisoprenes: test of tube dilation molecular picture. *Macromolecules* **33**, 499–506.

Mead, D. W., Larsen, R. G. & Doi, M. 1978 A molecular theory for fast flows of entangled polymers. *Macromolecules* **31**, 7895–7914.

Milner, S. T., McLeish, T. C. B. & Likhtman, A. E. 2001 Microscopic theory of convective constraint release. *J. Rheol.* **45**, 539–563.

Minegishi, A., Nishioka, A., Takahashi, T., Masubuchi, Y., Takimoto, J. & Koyama, K. 2001 Uniaxial elongational viscosity of PS/a small amount of UHMW-PS blends. *Rheol. Acta* **40**, 329–338.

Staudinger, H. 1932 *Die Hochmoleculuren organischen Kautschuk und Cellulose*. Springer.

Takimoto, J.-I., Tasaki, H. & Doi, M. 2000 Predictions of the rheological properties of polymer melts by stochastic simulation. In *Proc. XIIIth Int. Congr. Rheology, Cambridge, UK, August 2000*, vol. 2, pp. 97–99. Glasgow: British Society of Rheology.

Discussion

P.-G. DE GENNES (*Collège de France, Paris, France*). Your model assumes that all entanglements are constructed with two chains. Could there be some entanglements which involve three chains (or more)?

M. DOI. There are entanglements involving three or more chains, but we do not know how many there are and how important they are in rheological properties. At this stage, we are trying to go as far as possible with the assumption that entanglements are binary. By comparing the predictions of this model with experiments in detail, we can test the validity of this assumption. So far the binary entanglement model seems be sufficient to reproduce experimental results.

R. MAGERLE (*Physikalische Chemie II, Universität Bayreuth, Germany*). You mentioned that your model uses realistic distribution of molecular weights as inputs. How well does your model describe the behaviour of a set of the same polymer with different distribution of molecular weights?

M. DOI. We have demonstrated that the elongational viscosities of polystyrene samples with different molecular weight distributions can be described well by a single set of parameters.

A. N. SEMENOV (*Department of Applied Mathematics, University of Leeds, UK*). What is the dependence of the total number of entanglements on the shear rate?

M. DOI. The number of entanglements decreases with increasing shear rate (due to convective constraint release), and the decrease is stronger for longer molecules. We have not yet analysed the dependence in detail.

D. J. READ (*Department of Applied Mathematics, University of Leeds, UK*). How does the slip-link model relate to the tube model in the nonlinear regime? If slip links are further apart, does this mean the tube diameter changes? What happens to the tube diameter?

M. DOI. As mentioned above, the number of slip links decreases by flow in the nonlinear regime. This can be interpreted as an increase in the tube diameter, but this statement can be misleading since the 'tube diameter' has different meanings in different contexts. We hesitate to make such an interpretation.

M. E. CATES (*School of Physics, University of Edinburgh, UK*). Does your model give a monotonic flow curve $\sigma(\dot{\gamma})$ or does it give a maximum as predicted by early entanglement theories? If it is monotonic, it would be interesting to couple your algorithm to reversible breaking dynamics for chains. This would give a model for worm-like micelles which appear to have a non-monotonic flow curve, unlike conventional polymers.

M. DOI. Our model gives monotonic flow curves. It is quite interesting to extend this model to the worm-like micelles introducing the reversible breaking dynamics. If the extended model were to show the stress maximum in shear flow, it will be spectacular.

X. H. ZHENG (*Department of Pure and Applied Physics, Queen's University, Belfast, UK*). In the tube model some molecules play the role of tubes and others pass through

the tubes. What determines the population of these two kinds of molecules? Is it the free energy of the ensemble that determines the population of these two species?

M. DOI. In our dual slip-link model, all molecules play the role of both the tubes and the chains reptating in the tubes.